THEORETICAL AND APPLIED MECHANICS
Volume 42 (2015) Issue 4, 223–248 DOI: 10.2298/TAM1504223C

HIGHER-ORDER GRADIENT ELASTICITY MODELS APPLIED TO GEOMETRICALLY NONLINEAR DISCRETE SYSTEMS

Noël Challamel, Attila Kocsis, and C. M. Wang

This paper is dedicated to Academician Professor Teodor Atanacković, in honour of his 70^{th} birthday.

Abstract. The buckling and post-buckling behavior of a nonlinear discrete repetitive system, the discrete *elastica*, is studied herein. The nonlinearity essentially comes from the geometrical effect, whereas the constitutive law of each component is reduced to linear elasticity. The paper primarily focuses on the relevancy of higher-order continuum approximations of the difference equations, also called continualization of the lattice model. The pseudo-differential operator of the lattice equations are expanded by Taylor series, up to the second or the fourth-order, leading to an equivalent second-order or fourth-order gradient elasticity model. The accuracy of each of these models is compared to the initial lattice model and to some other approximation methods based on a rational expansion of the pseudo-differential operator. It is found, as anticipated, that the higher level of truncation is chosen, the better accuracy is obtained with respect to the lattice solution. This paper also outlines the key role played by the boundary conditions, which also need to be consistently continualized from their discrete expressions. It is concluded that higher-order gradient elasticity models can efficiently capture the scale effects of lattice models.

1. Introduction

Euler [19, 20] gave the exact buckling load for a pinned ended, inextensible, elastic column under a compressive axial load (see Oldfather et al. [39]). Lagrange [34] obtained the geometrically nonlinear exact equations of the problem and integrated the elliptic integral using asymptotic expansion formula. Lagrange [34] also investigated the higher-order buckling modes of simply supported inextensible elastic columns. Various *elastica* solutions are available for general boundary

2010 *Mathematics Subject Classification:* 39-XX; 74-XX; 34-XX; 65-XX; 06-XX.
Key words and phrases: elastica, post-buckling, lattice model, geometrical nonlinearity, discrete model, finite difference method, Hencky's chain, nonlocality, asymptotic expansion, gradient elasticity, higher-order differential model.

conditions and they are reported by Born [8], Love [37], Frisch-Fay [22], Antman [3] or Atanackovic [5] among others. Kuznetsov and Levyakov [33] recently investigated this *elastica* problem extensively and characterized the stability of the post-bifurcation branches.

The *elastica* problem, as already investigated by Euler [19] for the continuous case, can be formulated using a discrete version, also referred to as a discrete *elastica*. The linearized discrete *elastica* has been studied only in the beginning of the 1900s by Hencky [27] who considered a chain comprising elastically connected rigid links. Hencky [27] gave the buckling solutions of the finite problem for a number of links n such as $n = 2$, $n = 3$ and $n = 4$. Hencky [27] also observed that the continuous *elastica* problem may be obtained from considering an infinite number n of rigid links. The exact solution of this problem for arbitrary number of links was analytically given by Wang [52, 53], who solved a boundary value problem of second-order linear difference equations, whose solutions may be available in standard textbooks (such as Goldberg [25]). Silverman [46] remarked that this Hencky bar problem was mathematically equivalent to the finite difference formulation of the continuous problem when the length of the rigid link is made equal to the space discretization. Recently, Challamel et al. [12] showed that this discrete problem was mathematically similar to the vibrations equations of a discrete string, whose exact solution was first given by Lagrange [35].

The discrete *elastica* in a geometrically exact framework is a recent field which has emerged in the 1980s due to the interest of the research community in numerical and theoretical aspects of structural mechanics modelling (see for instance El Naschie et al. [17] or Gáspár and Domokos [23]). El Naschie et al. [17] numerically quantified the initial post-buckling curvature of the Hencky-bar system and compared the response with the local continuous problem. Gáspár and Domokos [23] showed an unexpected rich behaviour of the bifurcation diagram for the discrete *elastica*, which is not known for its continuum analogous. In fact, Gáspár and Domokos [23], Domokos [14] or Domokos and Holmes [15] pointed out possible spatial chaotic behavior of the Hencky bar-chain, a phenomenon originated from the discreteness of the system. The mathematical equivalence of the finite difference formulation of the Euler problem and the Hencky bar system has been shown in the linear range (Silverman [46]) and the equivalence can be also extended to the nonlinear range (Domokos and Holmes [15]). Wang [54] revisited the study on the post-buckling behaviour of the Hencky-bar chain for various boundary conditions. More recently, Kocsis and Károlyi [28, 29] observed spatial chaotic behaviour for discrete systems under non-conservative loads.

As mentioned by Bruckstein et al. [10], *elastica* curves may be also labelled as nonlinear splines in an industrial context and have found industrial applications in the field of computer graphics, or shape completion curves in image analysis. In this context, Brusckstein et al. [10] numerically solved some discrete *elastica* problems with various boundary conditions and additional constraints, and compared the solution with respect to the local one (for infinite number of fictitious links). The discrete *elastica* can be viewed as a numerical spatial discretization of a continuous rod problem (Bergou et al. [7]) or the investigation of a true discrete

mechanics problem (or lattice problem) that converges towards the continuous one at the limit. When considering the discretization problem, an important feature is the energy preserving property of the discrete spatial schemes. The discrete *elastica* investigated herein is introduced from an energy functional and it has energy preserving property. To the authors' knowledge, the corresponding second-order nonlinear difference equation has no available analytical solution although some approximate asymptotic solutions have been recently obtained by Challamel et al. [13]. We mention that alternative discrete schemes have been presented in the literature, which converge differently towards the continuous Euler *elastica*. Sogo [47] established a discrete scheme for the discrete *elastica*, related to the discrete Sine–Gordon equation (widely investigated for nonlinear wave propagation phenomena - see Braun and Kivshar [9]), with possible exact solution of the nonlinear lattice model. This scheme, however, differs from Hencky's system, as we shall discuss later. Kocsis [31] developed a section-based model for planar *Cosserat* rods, which can be applied as an alternative discrete mechanical model to the *elastica*, and which also differs from the *Hencky* chain.

In this paper, the discrete *elastica* will be investigated numerically and through an enriched continuum (or quasi-continuum) obtained by a continualization procedure. The continualization process approximates the finite difference operators of the lattice model by differential operators using Taylor-based expansion (Kruskal and Zabusky [32]) or rational-based expansion (Rosenau [42]). This methodology has been applied to the so-called FPU system, a nonlinear elastic axial chain with nonlinear restoring force studied by Fermi et al. [21]. The reader can refer to Maugin [38] for a historical perspective on the link between the Fermi-Pasta-Ulam lattice model (FPU system) and the continualized wave propagation equation. Kruskal and Zabusky [32] used a Taylor expansion of the second-order finite difference operator arising in the discrete lattice up to the fourth-order spatial derivative. The work of Triantafyllidis and Bardenhagen [49] may be mentioned for the static behaviour of a nonlinear elastic axial chain (including FPU chain) and its link to gradient elasticity model using Taylor asymptotic expansion of the difference operators. Triantafyllidis and Bardenhagen [49] applied continualization to the governing equations and to the energy functional.

We have recently shown from a rational expansion that the discrete elastica may behave as a nonlocal continuous elastica, both in the buckling (Wang et al. [51]; Challamel et al. [11]) and the post-buckling regimes (Challamel et al. [13]). The nonlocality is here understood as an Eringen's type nonlocality or stress gradient model (Eringen [18]). This nonlocal model has been considered for bending of nonlocal beams by Peddieson et al. [41] (see also Sudak [48]). Eringen's model applied at the beam scale may be formulated from the lattice spacing of Hencky bar chain model:

$$M - \frac{a^2}{12}\frac{d^2M}{ds^2} = EI\kappa \tag{1.1}$$

where M is the bending moment, EI is the bending stiffness, κ is the curvature and a is the lattice spacing with $a = L/n$ for a beam of length L composed of n

rigid links. The nonlocal length scale has been identified from the lattice spacing; thereby giving a kind of physical support for justifying nonlocal beam mechanics.

In this paper, we explore a gradient-type curvature driven law, first expressed by the second-order curvature constitutive law:

$$M = EI\left[\kappa + \frac{a^2}{12}\frac{d^2\kappa}{ds^2}\right] \tag{1.2}$$

and then we shall investigate a higher-order gradient constitutive law given by:

$$M = EI\left[\kappa + \frac{a^2}{12}\frac{d^2\kappa}{ds^2} + \frac{a^4}{360}\frac{d^4\kappa}{ds^4}\right] \tag{1.3}$$

It will be shown that the pseudo-differential operator of the lattice equations can be expanded by Taylor expansions, up to the second or fourth-order, leading to an equivalent second-order or fourth-order gradient model. The accuracy of each of these models is compared first to the initial lattice model and then to some other approximation methods based on a rational expansion of the pseudo-differential operator. It is found, as anticipated, that when a higher level of truncation is chosen, a better accuracy is achieved with respect to the lattice solution. The key role played by the boundary conditions is also outlined, which need to be consistently continualized from their discrete expression. Higher-order gradient elasticity models can efficiently capture the scale effects of lattice models.

2. Discrete elastica

Consider a Hencky's bar-chain (or discrete elastica system) with pinned-pinned ends as shown in Figure 1. The column, composed of n repetitive cells of size a, is axially loaded by a concentrated force denoted by P. The discrete column of length L is modelled by some finite rigid segments and elastic rotational springs of stiffness $k = EI/a$, where EI is the bending rigidity of the local Euler-Bernoulli column asymptotically obtained for an infinite number n of rigid links.

It is possible to introduce the energy function of this problem as:

$$\begin{aligned} U = \sum_{i=1}^{n-1} \frac{EI}{4}\left[\left(\frac{\theta_{i+1}-\theta_i}{a}\right)^2 + \left(\frac{\theta_i-\theta_{i-1}}{a}\right)^2\right] \times a \\ + \frac{EI}{4}\left(\frac{\theta_1-\theta_0}{a}\right)^2 \times a + \frac{EI}{4}\left(\frac{\theta_n-\theta_{n-1}}{a}\right)^2 \times a - P \times a \sum_{i-1}^{n-1}(1-\cos\theta_i) \end{aligned} \tag{2.1}$$

which can be equivalently reformulated as:

$$U = \sum_{i=0}^{n} \frac{EI}{2}\left(\frac{\theta_{i+1}-\theta_i}{a}\right)^2 \times a - P \times a \sum_{i=1}^{n-1}(1-\cos\theta_i)$$

The stationarity of this energy function $\delta U = 0$ leads to the nonlinear difference equation of the discrete *elastica*:

$$EI\frac{\theta_{i+1} - 2\theta_i + \theta_{i-1}}{a^2} + P\sin\theta_i = 0 \tag{2.2}$$

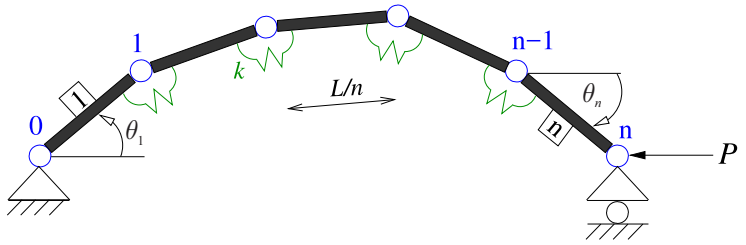

FIGURE 1. Hencky's chain: n rigid links are connected by hinges and rotational springs.

The discrete *elastica* equations can be equivalently obtained from the following system of nonlinear difference equations:

$$M_i = EI\frac{\theta_{i+1}-\theta_i}{a} \quad \text{and} \quad \frac{M_i - M_{i-1}}{a} + P\sin\theta_i = 0 \tag{2.3}$$

Here M_i is the bending moment in the rotational spring at hinge i, and θ_i is the angle of the i^{th} link from the line of action of compressive force P. In other words, θ_i is the rotation angle of the segment i connecting the $(i-1)^{\text{th}}$ node and the i^{th} node.

As pointed out by Domokos and Holmes [15], the difference equations (2.3) can be obtained from the differential equation system of the axially compressed, hinged-hinged elastica, $M = EI \times d\theta/ds$ and $dM/ds + P\sin\theta = 0$, by using forward and backward differences, respectively. This yields a semi-implicit Euler method, which defines an area preserving map. It is worth mentioning that, except the discussion on boundary conditions, the discrete *elastica* may be equivalently obtained from the centred finite difference scheme expressed by:

$$M_i = EI\frac{\theta_{i+1/2}-\theta_{i-1/2}}{a} \quad \text{and} \quad \frac{M_{i+1/2} - M_{i-1/2}}{a} + P\sin\theta_i = 0$$

To the authors' knowledge, there is no available analytical solution for Eq. (2.2) in the literature. Sogo [47] used an alternative scheme, also introduced via variational arguments, which may be expressed as

$$4EI\frac{\sin\left(\frac{\theta_{i+1}-\theta_i}{2}\right) - \sin\left(\frac{\theta_i-\theta_{i-1}}{2}\right)}{a^2} + P\left[\sin\left(\frac{\theta_i+\theta_{i-1}}{2}\right) + \sin\left(\frac{\theta_i+\theta_{i+1}}{2}\right)\right] = 0 \tag{2.4}$$

Equation (2.4) may alternatively be written as:

$$4\frac{EI}{a^2}\sin\left(\frac{\theta_{i+1}-2\theta_i+\theta_{i-1}}{4}\right) + P\sin\left(\frac{\theta_{i-1}+2\theta_i+\theta_{i+1}}{4}\right) = 0 \tag{2.5}$$

Sogo [47] obtained a closed-form solution for Eq. (2.5) by using elliptic functions. Although Eq. (2.5) and Eq. (2.2) are different, both converge towards the continuous *elastica* for $a \to 0$ (or $n \to \infty$):

$$EI\theta'' + P\sin\theta = 0$$

The nonlinear difference equation (2.2) of the elastica can be reformulated in a dimensionless form:

$$\theta_{i+1} - 2\theta_i + \theta_{i-1} = -\frac{\beta}{n^2}\sin\theta_i \tag{2.6}$$

by using the dimensionless load $\beta = PL^2/EI$. The nonlinear difference equation can be equivalently reformulated with the following relations

$$\theta_{i+1} = \theta_i + \frac{\hat{\kappa}_i}{n} \quad \text{and} \quad \hat{\kappa}_{i+1} = \hat{\kappa}_i - \frac{\beta}{n}\sin\theta_{i+1}$$

where the dimensionless curvature $\hat{\kappa}_i$ is defined as $\hat{\kappa}_i = L\kappa_i$ and the curvature $\kappa_i = M_i/EI$ (see Challamel et al. [13]). The boundary conditions of the pinned-pinned column are obtained from the vanishing of the bending moments at both ends, i.e. $M_0 = 0$ and $M_n = 0$:

$$\theta_1 = \theta_0 \quad \text{and} \quad \theta_{n+1} = \theta_n \tag{2.7}$$

The analytical solution for the fundamental buckling load on the basis of the linearization process, was calculated by Wang [52, 53] (see more recently by Challamel et al. [12]) for arbitrary number of links n. The reasoning is briefly presented below. The linearization of Eq. (2.6) for computing the buckling load gives:

$$\theta_{i+1} + \left(\frac{\beta}{n^2} - 1\right)\theta_i + \theta_{i-1} = 0$$

The solution of this linear difference boundary value problem can be expressed with the real basis as (Challamel et al. [13]):

$$\theta_i = A\cos(\phi i) + B\sin(\phi i) \quad \text{with} \quad \phi = \arccos\left(1 - \frac{\beta}{2n^2}\right) \tag{2.8}$$

The substitution of Eq. (2.8) into the first boundary condition given in Eq. (2.7) (i.e. $\theta_1 = \theta_0$) leads to the following buckling mode:

$$\theta_i = \theta_0 \frac{\sin(\phi i) - \sin(\phi(i-1))}{\sin\phi} = \theta_0 \frac{cos\left(\phi i - \frac{\phi}{2}\right)}{\cos\frac{\phi}{2}}$$

Now, the consideration of the second boundary condition $\theta_{n+1} = \theta_n$ gives the k^{th} buckling load of the pinned-pinned Hencky chain:

$$\sin(\phi n) = 0 \;\Rightarrow\; \phi n = k\pi \;\Rightarrow\; \cos\frac{k\pi}{n} = 1 - \frac{\beta}{2n^2} \;\Rightarrow\; \beta_{\text{crit}} = 4n^2\sin^2\left(\frac{k\pi}{2n}\right)$$

The discrete boundary value problem defined by Eqs. (2.6) and (2.7) can be solved by using the shooting method (see for instance Kocsis [30]). The solutions form equilibrium paths and are shown in blue colour in Figure 2. As pointed out by Gáspár and Domokos [23], Domokos [14] or Domokos and Holmes [15], the discrete system possesses very rich structure inherent to the discrete property of the structural system. The discrete system possesses a multiplicity of solutions appearing from the primary branches in saddle node bifurcation, a property which is not observed for the continuous *elastica* system. These solutions are classified as parasitic solutions. As well described in Domokos and Holmes [15], the number of parasitic solutions increases with respect to the number of links n.

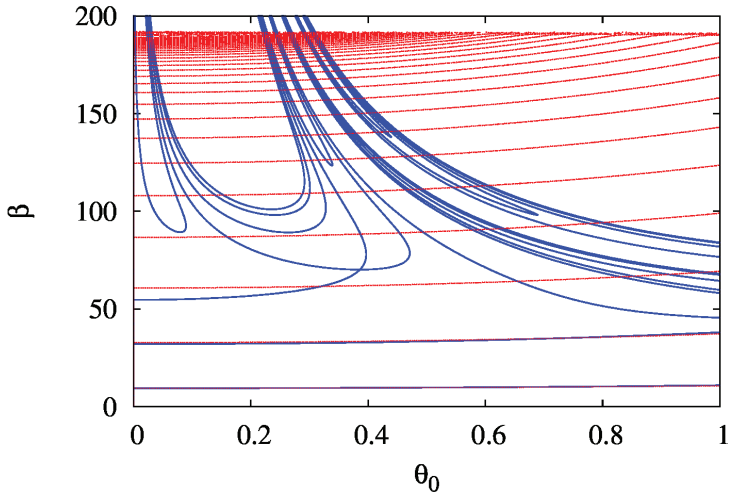

FIGURE 2. Bifurcation diagrams of the nonlocal elastica with local boundary conditions (red) for $n = 4$ and the Hencky chain of 4 links (blue). The relative rotation of neighbouring links in the Hencky chain is less than 2π.

3. Higher-order elasticity by continualization method

Now, a continuous approximation of the discrete elastica will be expressed by using a so-called continualization approach. The nonlinear difference equations can be continualized starting from the following relations between the discrete and equivalent continuous systems $\theta_i = \theta(s = ia)$ for a sufficiently smooth deflection function:

$$\theta(s+a) = \sum_{k=0}^{\infty} \frac{a^k d_s^k}{k!}\theta(s) = e^{ad_s}\theta(s) \quad \text{with} \quad d_s = \frac{d}{ds}$$

The methodology that aims to approximate a discrete system by a continuous one is called a continualization procedure or the method of differential approximation (Shokin [45]). The method involves finding the best enriched continuum associated with a discrete model (or lattice model) and is based on the asymptotic expansion of the difference operators using Taylor-based or some other asymptotic expansion. By introducing the pseudo-differential Laplacian operator

$$\frac{\theta_{i-1} + \theta_{i+1} - 2\theta_i}{a^2} = \frac{\left[e^{ad_s} + e^{-ad_s} - 2\right]}{a^2}\theta(s) = \frac{4}{a^2}\sinh^2\left(\frac{a}{2}d_s\right)\theta(s)$$

one obtains the following system of pseudo-differential equations for *discrete elastica* problem defined by Eq. (2.2):

$$4\frac{EI}{a^2}\sinh^2\left(\frac{a}{2}d_s\right)\theta + P\sin\theta = 0$$

A fourth-order Taylor-based asymptotic expansion of this pseudo differential operator leads to:

$$\frac{4}{a^2}\sinh^2\left(\frac{a}{4}d_s\right) = d_s^2 + \frac{a^2}{12}d_s^4 + \frac{a^4}{360}d_s^6 + o(a^6)\dots$$

The coefficients of the fourth-order asymptotic expansion were already given by Rosenau [43], Wattis [55] or Askes et al. [4]. A similar second-order Taylor-based asymptotic expansion was applied by Kruskal and Zabusky [32] for a nonlinear discrete axial chain.

The second-order gradient elasticity model associated with the discrete *elastica* then yields:

$$EI\left(\theta'' + \frac{a^2}{12}\theta^{(4)}\right) + P\sin\theta = 0 \tag{3.1}$$

whereas the fourth-order gradient elasticity model is obtained from a higher-order asymptotic expansion:

$$EI\left(\theta'' + \frac{a^2}{12}\theta^{(4)} + \frac{a^4}{360}\theta^{(6)}\right) + P\sin\theta = 0 \tag{3.2}$$

The prime denotes the spatial differentiation with respect to the curvilinear abscissa, i.e. $d_s\theta = \theta'$. In order to avoid higher-order derivatives, and due to the specific property of the energy functional of these continualized models, a rational-based asymptotic expansion has been also used in the literature (see for instance Rosenau [42], Wattis [55], Andrianov et al. [1, 2] for axial wave applications):

$$\frac{4}{a^2}\sinh^2\left(\frac{a}{2}d_s\right) = \frac{d_s^2}{1-\frac{a^2}{12}d_s^2} + \dots$$

Such a Padé approximation of the pseudo-differential operator leads to a second-order nonlinear differential equation:

$$EI\theta'' + P\sin\theta - P\frac{a^2}{12}(\sin\theta)'' = 0$$

which is strictly equivalent to

$$\left(EI - P\frac{a^2}{12}\cos\theta\right)\theta'' + P\left(1 + \frac{a^2}{12}\theta'^2\right)\sin\theta = 0 \tag{3.3}$$

This last model can be classified as a nonlocal model of Eringen's type applied at the beam scale. In this paper, we will explore the capability of these three higher-order models (approximated differential models or quasi-continuum models) to capture the scale effects of the exact discrete *elastica* (or Hencky chain model).

4. Overview of nonlocal and discrete *elastica*

There is a strict equivalence between the nonlinear differential equation (3.3) and the nonlocal moment gradient elasticity model of Eringen's type as applied to the beam and the governing equations may be written as:

$$M - l_c^2 M'' = EI\theta' \quad \text{and} \quad M' + P\sin\theta = 0 \quad \text{with} \quad l_c^2 = \frac{a^2}{12} \tag{4.1}$$

The first equation in Eq. (4.1) is exactly Eq. (1.1). In other words, the continualization of the discrete *elastica* based on a rational expansion of the pseudo-differential operator is equivalent to the formulation of a nonlocal *elastica*, where the length scale is calibrated with respect to the cell size of the Hencky bar system. The nonlocality here arises as the stress gradient model of Eringen [18] as applied at the beam scale. The nonlocal *elastica*, where nonlocality is of Eringen's type, has been recently investigated in details by Wang et al. [50], Shen [44], Xu et al. [56] or Challamel et al. [13] for small scale structure applications. Atanackovic et al. [6] found some new solutions for the optimization of nonlocal elastic columns.

For the continualized problem investigated herein, consistent continualized boundary conditions should be considered as the continualization of the discrete ones Eq. (2.7):

$$\theta(a) = \theta(0) \quad \text{and} \quad \theta(L+a) = \theta(L) \tag{4.2}$$

The following dimensionless parameters can be introduced as well:

$$\beta = \frac{PL^2}{EI}, \quad \xi = \frac{s}{L} \quad \text{and} \quad \hat{l}_c = \frac{l_c}{L}$$

The *nonlocal elastica* is then reduced to the resolution of the nonlinear second-order differential equation expressed in dimensionless format:

$$\left(1 - \beta \hat{l}_c^2 \cos\theta\right) \frac{d^2\theta}{d\xi^2} + \beta \left[1 + \hat{l}_c^2 \left(\frac{d\theta}{d\xi}\right)^2\right] \sin\theta = 0$$

which can be converted into a first order differential equation system:

$$\frac{d\theta}{d\xi} = \hat{\kappa} \quad \text{and} \quad \frac{d\hat{\kappa}}{d\xi} = -\beta \sin\theta \frac{1 + \hat{l}_c^2 \hat{\kappa}^2}{1 - \beta \hat{l}_c^2 \cos\theta} \tag{4.3}$$

The boundary value problem defined by Eq. (4.3) with nonlocal boundary conditions Eq. (4.2) can be solved numerically, as thoroughly discussed in Challamel et al. [13]. The bifurcation diagrams of the discrete and nonlocal elastica (with uncentred nonlocal boundary conditions) are shown in Figures 4 and 5. For comparison studies, results are also reported for the nonlocal problem with "local" centred boundary conditions, given in a non-dimensional format as:

$$\frac{d\theta}{d\xi}(0) = 0 \quad \text{and} \quad \frac{d\theta}{d\xi}(1) = 0$$

Figure 2 shows the bifurcation diagram of the nonlocal elastica with local boundary conditions for $n = 4$, and that of the discrete elastica (*Hencky* chain) of 4 links. Solutions where the relative rotation between neighbouring links of the *Hencky* chain exceeds 2π are not shown. Figure 3 shows the first three bifurcation branches of these models. Figure 4 shows the bifurcation diagram of the nonlocal elastica with nonlocal boundary conditions for $n = 4$, and that of the *Hencky* chain of 4 links, while Figure 5 shows the first three bifurcation branches of these two models. It is clear that the nonlocal model is efficient in capturing the primary bifurcation branch up to large rotation values but it fails to capture the higher-order branches. This observation is also detailed in Table 1. Furthermore, the need of

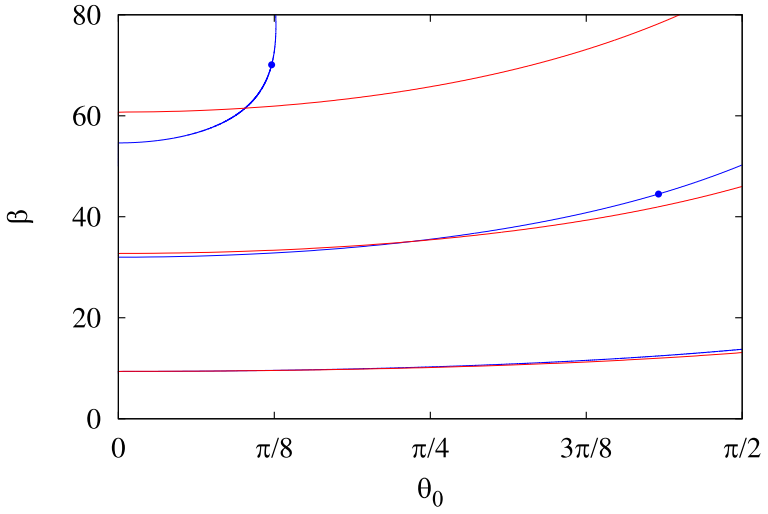

FIGURE 3. The first three paths of the the *Hencky* chain (blue) and the first three paths of the nonlocal *elastica* with local boundary conditions (red) for $n = 4$. Bifurcation points of the paths are denoted.

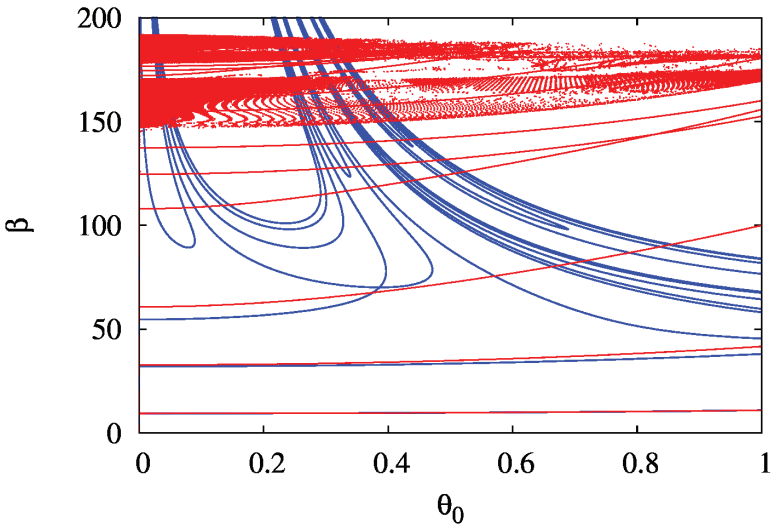

FIGURE 4. Bifurcation diagrams of the nonlocal *elastica* with nonlocal boundary conditions (red) for $n = 4$ and the *Hencky* chain of 4 links (blue). The relative rotation of neighbouring links in the Hencky chain is less than 2π.

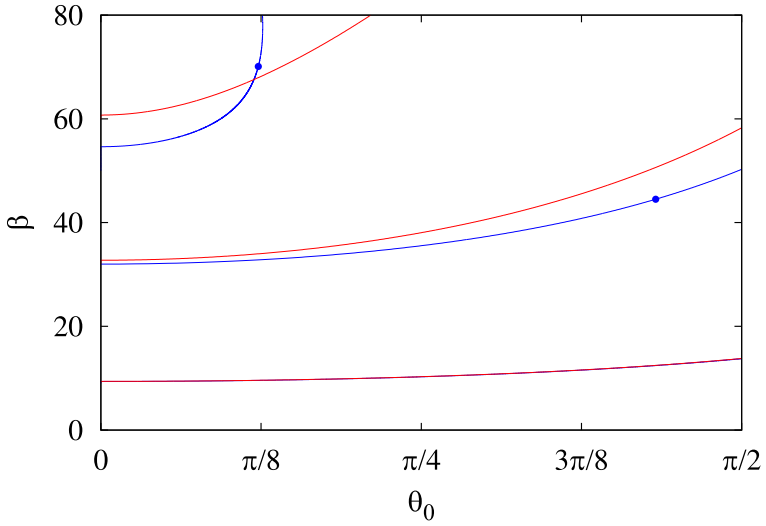

FIGURE 5. The first three paths of the the *Hencky* chain (blue) and the first three paths of the nonlocal *elastica* with nonlocal boundary conditions (red) for $n = 4$. Bifurcation points of the paths are denoted.

introducing uncentred nonlocal boundary conditions is confirmed by the numerical comparison of each nonlocal model and the reference lattice one. A closed-form solution of the buckling load can be easily obtained for the nonlocal *elastica* with centred or uncentred boundary conditions. For centred boundary conditions, the buckling mode can be obtained as (Challamel et al. [13]):

$$\theta(\xi) = \theta_0 \cos \pi\xi \;\Rightarrow\; \beta = \frac{\pi^2}{1 + \pi^2 \frac{l_c^2}{L^2}} \quad \text{with} \quad l_c^2 = \frac{a^2}{12}$$

whereas for uncentred boundary conditions, the buckling mode is similar to the one of the discrete problem that has been continualized, and leads to the same buckling value obtained with the centred boundary conditions:

$$\theta(\xi) = \theta_0 \frac{\cos\left[\pi\left(\xi - \frac{a}{2L}\right)\right]}{\cos \frac{\pi a}{2L}} \;\Rightarrow\; \beta = \frac{\pi^2}{1 + \pi^2 \frac{l_c^2}{L^2}} \quad \text{with} \quad l_c^2 = \frac{a^2}{12}$$

5. Second-order gradient elasticity models

Considering the Taylor-based asymptotic expansion of the pseudo-differential operator, the nonlinear differential equation associated with a second-order gradient elasticity model given by Eq. (3.1) is now investigated. This gradient elasticity model has been obtained from continualization of the governing equations, but it is also possible to continualize directly the energy function given in Eq. (2.1) by

TABLE 1. Computation of first stable bifurcation branch $\beta = f(\theta_0)$ in case of $n = 4$; Local boundary conditions characterized by $\theta'(0) = \theta'(L) = 0$; Uncentred nonlocal boundary conditions characterized by $\theta(a) - \theta(0) = 0$ and $\theta(an + a) - \theta(an) = 0$; centered higher-order boundary conditions obtained from $\theta'(0) = \theta'(L) = 0$ and $\theta'''(0) = \theta'''(L) = 0$.

$\theta(0) = \theta_0$	0	0.25	0.5	0.75	1
β (Hencky system)	$4n^2 \sin^2 \frac{\pi}{2n} \approx 9.3726$	9.4589	9.7241	10.1883	10.8885
β (nonlocal method; local boundary conditions)	$\frac{\pi^2}{1+\pi^2/(12n^2)} \approx 9.3871$	9.4608	9.6872	10.0825	10.6772
β (nonlocal method; uncentred nonlocal boundary conditions)	$\frac{\pi^2}{1+\pi^2/(12n^2)} \approx 9.3871$	9.4735	9.7393	10.2043	10.9067
β (2^{nd} order gradient elasticity method; centred boundary conditions)	$\pi^2\left(1-\frac{\pi^2}{12n^2}\right) \approx 9.3623$	9.4358	9.6618	10.0572	10.6541
β (2^{nd} order gradient elasticity method; uncentred boundary conditions)	$\pi^2\left(1-\frac{\pi^2}{12n^2}\right) \approx 9.3623$	9.4484	9.7134	10.1770	10.8767
β (4^{th} order gradient elasticity method; centred boundary conditions)	$\pi^2\left(1-\frac{\pi^2}{12n^2}+\frac{\pi^4}{360n^4}\right) \approx 9.3727$	9.4463	9.6725	10.0675	10.6621
β (4^{th} order gradient elasticity method; uncentred boundary conditions)	$\pi^2\left(1-\frac{\pi^2}{12n^2}+\frac{\pi^4}{360n^4}\right) \approx 9.3727$	9.4590	9.7242	10.1886	10.8898

$\theta(0) = \theta_0$	1.25	1.5	1.75	2
β (Hencky system)	11.8856	13.2771	15.2219	17.9929
β (nonlocal method; local boundary conditions)	11.5216	12.6975	14.3420	16.6955
β (nonlocal method; uncentred nonlocal boundary conditions)	11.9092	13.3149	15.2969	18.1626
β (2^{nd} order gradient elasticity method; centred boundary conditions)	11.5080	12.7145	14.4501	17.0855
β (2^{nd} order gradient elasticity method; uncentred boundary conditions)	11.8737	13.2686	15.2262	18.0342
β (4^{th} order gradient elasticity method; centred boundary conditions)	11.5073	12.6861	14.3372	16.7040
β (4^{th} order gradient elasticity method; uncentred boundary conditions)	11.8910	13.2959	15.2804	18.1632

using the following energy functional:

$$U = \int_0^L \frac{EI}{4}\left[\left(\frac{\theta(x+a)-\theta(x)}{a}\right)^2 + \left(\frac{\theta(x)-\theta(x-a)}{a}\right)^2\right] - P(1-\cos\theta)dx$$
$$= \int_0^L \frac{EI}{4}\left[\left(\theta' + \frac{a}{2}\theta'' + \frac{a^2}{6}\theta'''\right)^2 + \left(\theta' - \frac{a}{2}\theta'' + \frac{a^2}{6}\theta'''\right)^2 + o(a^4)\right] - P(1-\cos\theta)dx$$

where the boundary terms have been omitted. The internal energy functional can also be presented in the following simplified form

$$\pi^0 = \int_0^L \frac{EI}{2}\left[\theta'^2 + \frac{a^2}{4}\theta''^2 + \frac{a^2}{3}\theta'\theta''' + o(a^4)\right]dx$$
$$= \int_0^L \frac{EI}{2}\left[\theta'^2 - \frac{a^2}{12}\theta''^2\right]dx + \left[\frac{a^2}{3}\theta'\theta''\right]_0^L + o(a^4)$$

The continualized energy is not positive definite. The continualized model can be classified as a second-order gradient elasticity model with some negative contributions of the small length scale terms, as shown below:

$$U = \int_0^L \frac{EI}{2}\left(\theta'^2 - \frac{a^2}{12}\theta''^2\right) - P(1-\cos\theta)dx$$

The stationarity of this energy functional $\delta U = 0$ also leads to the same nonlinear differential equation as Eq. (3.1) with the following higher-order boundary conditions:

$$\left[-EI\frac{a^2}{12}\theta''\delta\theta'\right]_0^L + \left[EI\left(\theta' + \frac{a^2}{12}\theta'''\right)\delta\theta\right]_0^L = 0 \tag{5.1}$$

One recognizes a kind of gradient elasticity beam model with a negative sign affecting the small length scale contribution (as opposed to gradient elasticity models with positive definite energy - see Lazopoulos [36]; Papargyri-Beskou et al. [40]). Note also that the natural boundary condition in Eq. (5.1) may define the bending moment as:

$$M = EI\left(\theta' + \frac{a^2}{12}\theta'''\right)$$

Note that this equation is the same as Eq. (1.2). The second-order gradient elasticity model can be reformulated in a dimensionless nonlinear fourth-order differential equation:

$$\frac{d^2\theta}{d\xi^2} + \frac{1}{12n^2}\frac{d^4\theta}{d\xi^4} = -\beta\sin\theta \tag{5.2}$$

The centred boundary conditions of this second-order gradient elasticity model may be chosen from Eq. (5.1):

$$\theta'(0) = \theta'(L) = 0 \quad \text{and} \quad \theta'''(0) = \theta'''(L) = 0 \tag{5.3}$$

The uncentred boundary conditions obtained by continualization of the discrete-based boundary conditions Eq. (2.7) of this second-order gradient elasticity model are chosen as:

$$\theta'\left(\frac{a}{2}\right) = \theta'\left(L + \frac{a}{2}\right) = 0 \quad \text{and} \quad \theta'''\left(\frac{a}{2}\right) = \theta'''\left(L + \frac{a}{2}\right) = 0 \tag{5.4}$$

The following asymptotic expansion lies behind this uncentred boundary condition:

$$\begin{aligned} \theta(0) = \theta(a) \;&\Rightarrow\; \theta\left(\frac{a}{2} - \frac{a}{2}\right) = \theta\left(\frac{a}{2} + \frac{a}{2}\right) \\ &\Rightarrow\; \theta\left(\frac{a}{2}\right) - \frac{a}{2}\theta'\left(\frac{a}{2}\right) + \frac{1}{2}\left(\frac{a}{2}\right)^2\theta''\left(\frac{a}{2}\right) + \dots \\ &= \theta\left(\frac{a}{2}\right) + \frac{a}{2}\theta'\left(\frac{a}{2}\right) + \frac{1}{2}\left(\frac{a}{2}\right)^2\theta''\left(\frac{a}{2}\right) + \dots \end{aligned}$$

which implies that:

$$\theta'\left(\frac{a}{2}\right) = \theta'''\left(\frac{a}{2}\right) = 0$$

The reasoning is identical at the other boundary.

Eq. (5.2) can be transformed in a first order differential equation system:

$$\begin{aligned} \theta' &= \kappa \\ \kappa' &= \gamma \\ \gamma' &= \alpha \\ \alpha' &= -12n^2(\gamma + \beta\sin\theta) \end{aligned} \tag{5.5}$$

This ordinary differential equation system, written in the short form $\underline{x}' = \underline{f}(\underline{x})$, where $\underline{x} = [\theta, \kappa, \gamma, \alpha]^T$, can be solved numerically with the simplex algorithm. In case of centred boundary conditions, according to Eq. (5.3), the close-end boundary conditions are $\kappa_0 = 0$ and $\alpha_0 = 0$. There is one parameter, i.e. the load β, and there are two variables, i.e. θ_0 and γ_0. They span a 3D global representation space (GRS). For each point in this space Eq. (5.5) is solved by a time-stepping algorithm, where the dimensionless, unit rod length is discretized in m parts. It yields the far-end values of κ and α. Owing to the far-end boundary conditions, $\kappa_m = 0$ and $\alpha_m = 0$ should fulfill, and these are the error functions of the simplex scanning algorithm (Gáspár et al. [24]).

Figures 6 and 7 show the bifurcation diagrams for $n = 2, 3, 4, 5, 6$ and 7. The scanned domain of the global representation space is $\theta_0 \in (-1, 1)$, $\gamma_0 \in (-16\pi, 16\pi)$, and $\beta \in (0, 200)$. The grid of the GRS is $300 \times 5000 \times 2000$, while the rod is discretized in $m = 1000$ parts with a predictor-corrector time-stepping algorithm, which predicts the solution in the next time step with the Euler method and correct it with the second-order Adams-Moulton method (Hairer et al [26]). The output of the scanning algorithm is refined by the Newton-Raphson method. Figure 8 shows the bifurcation diagram of the second-order gradient elasticity model Eq. (5.2) with centred boundary conditions Eq. (5.3) for $n = 4$, and that of the Hencky chain of 4 links. Solutions where the relative rotation between neighbouring links of the Hencky chain exceeds 2π are not shown.

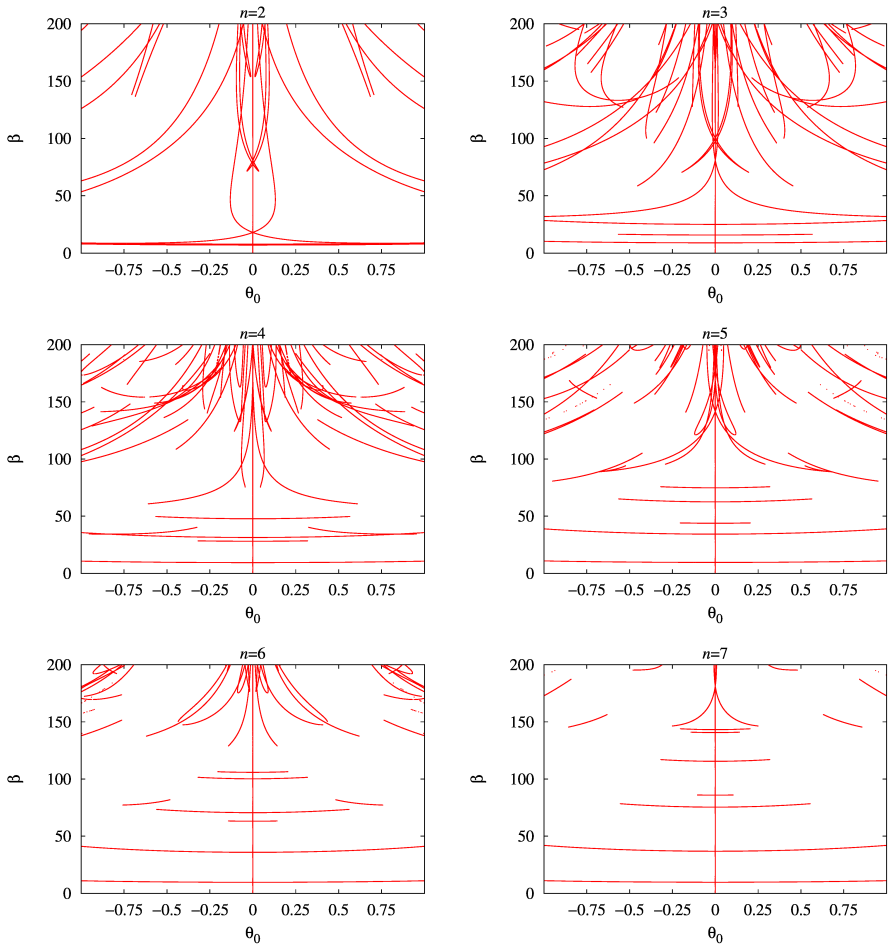

FIGURE 6. Bifurcation diagrams of the second-order gradient elasticity model, Eq. (5.2), with centred boundary conditions, Eq. (5.3), for $n = 2, 3, 4, 5, 6$ and 7. Projection of the equilibrium paths on the subspaces of (θ_0, β) are shown, the values of n are indicated on the top of the figures. The scanned domain of the global representation space is $\beta \in (0, 200)$, $\theta_0 \in (-1, 1)$ and $\gamma_0 \in (-16\pi, 16\pi)$, and the rod is discretized in $m = 1000$ parts with the stepping algorithm.

An equilibrium path can also be followed by the simplex algorithm (Domokos and Gáspár [16]). For that a known point on the path is required. The first three paths of the *Hencky* chain and the first four paths of the second-order gradient elasticity model Eq. (5.2) with centred boundary conditions Eq. (5.3) are computed for $n = 4$, starting from the corresponding bifurcation points of the trivial equilibrium path. These paths are shown in Figure 9. Note that the first paths of

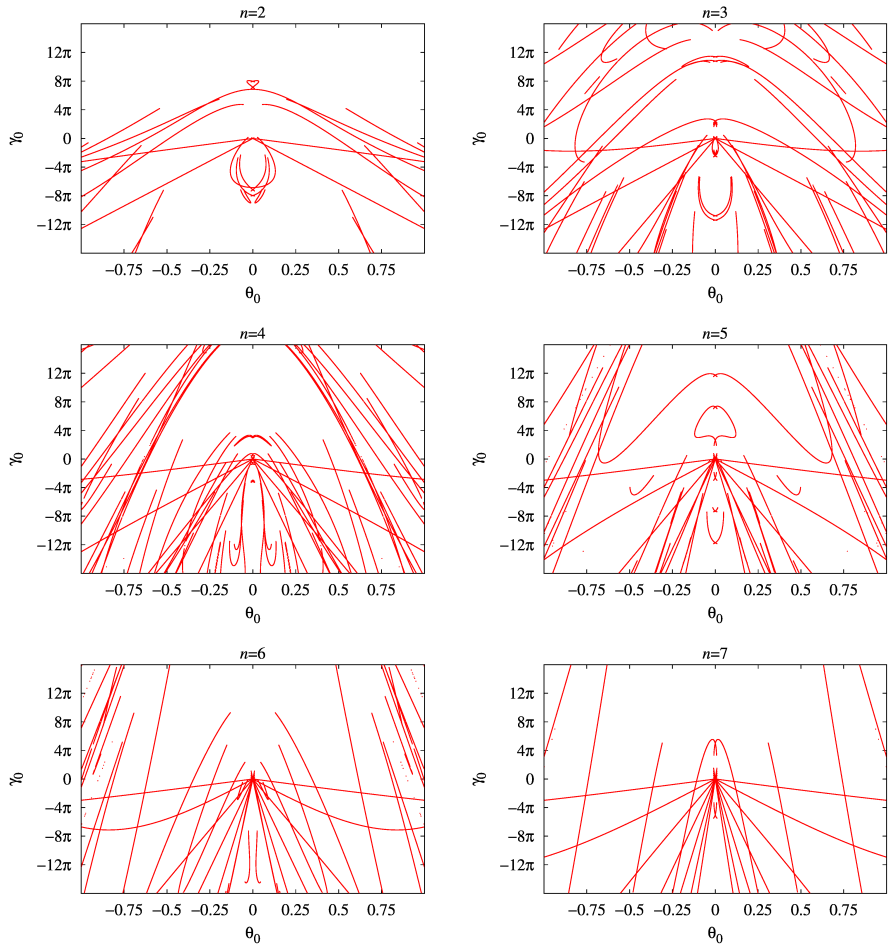

FIGURE 7. Bifurcation diagrams of the second-order gradient elasticity model, Eq. (5.2), with centred boundary conditions, Eq. (5.3), for $n = 2, 3, 4, 5, 6$ and 7. Projection of the equilibrium paths on the subspaces of θ_0, γ_0 are shown, the values of n are indicated on the top of the figures. The scanned domain of the global representation space is $\beta \in (0, 200)$, $\theta_0 \in (-1, 1)$ and $\gamma_0 \in (-16\pi, 16\pi)$, and the rod is discretized in $m = 1000$ parts in the stepping algorithm.

the two models are very close to each other. In this respect, the second-order gradient elasticity model with centred boundary conditions approximates the discrete model very well. However, the second path of the gradient elasticity model is far away from being a good estimate of the second path of the discrete model. Rather the third and the fourth paths of the gradient elasticity model seem to correspond better to the second and third paths of the discrete model.

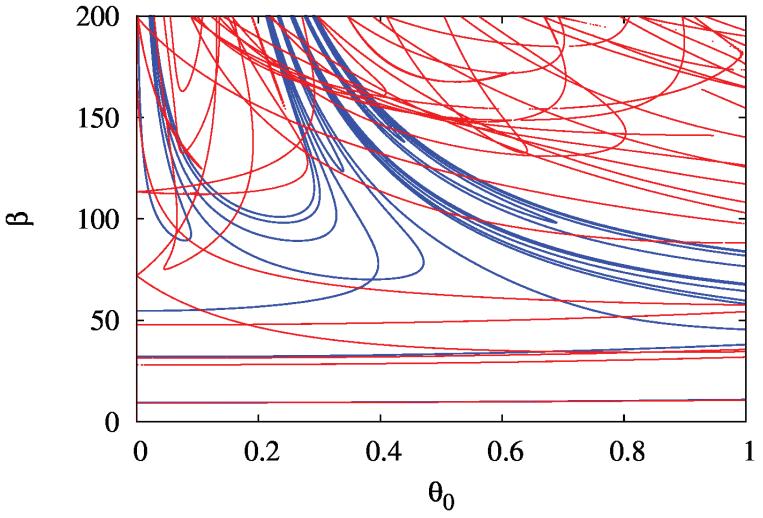

FIGURE 8. Bifurcation diagrams of the second-order gradient elasticity model with centred boundary conditions (red) for $n = 4$ and the *Hencky* chain of 4 links (blue). The relative rotation of neighbouring links in the *Hencky* chain is less than 2π.

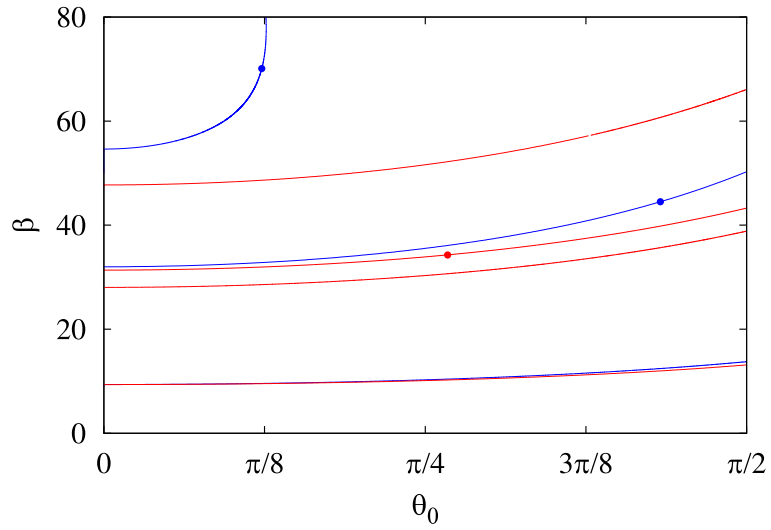

FIGURE 9. The first three paths of the the *Hencky* chain (blue) and the first four paths of the second-order gradient elasticity model with centred boundary conditions (red) for $n = 4$. Bifurcation points of the paths are denoted.

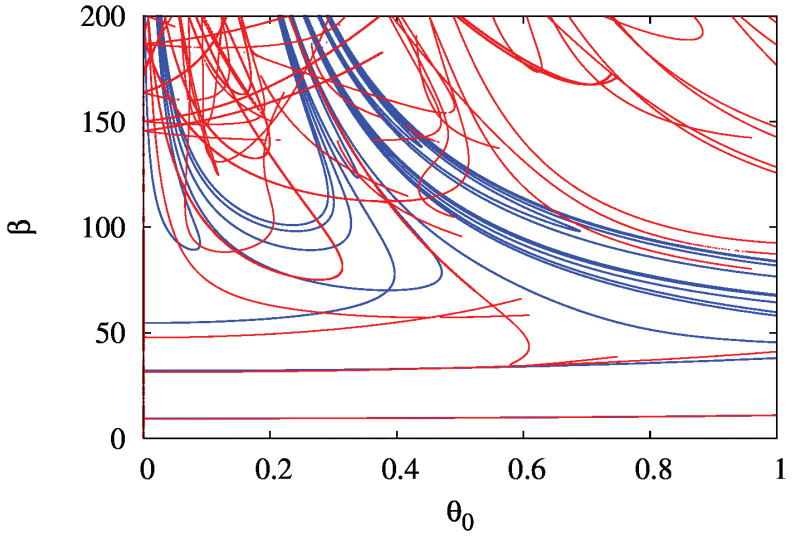

FIGURE 10. Bifurcation diagrams of the second-order gradient elasticity model with uncentred boundary conditions (red) for $n = 4$ and the *Hencky* chain of 4 links (blue). The relative rotation of neighbouring links in the Hencky chain is less than 2π.

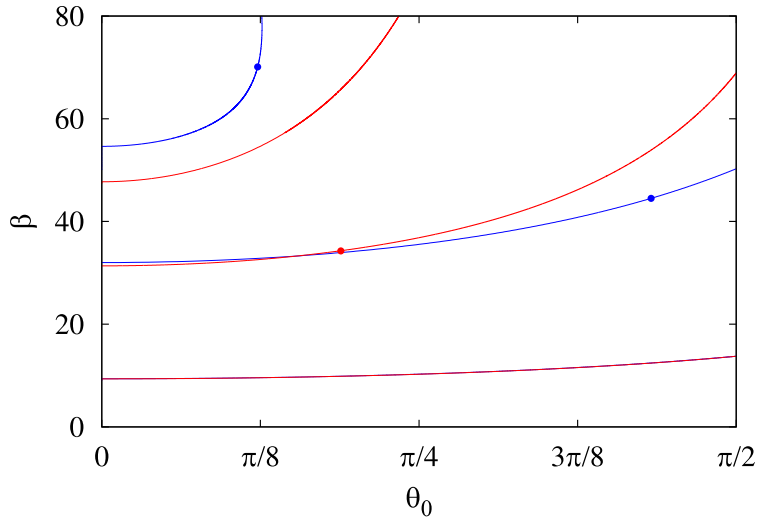

FIGURE 11. The first three paths of the the *Hencky* chain (blue) and the first three paths of the second-order gradient elasticity model with uncentred boundary conditions (red) for $n = 4$. Bifurcation points of the paths are denoted.

The uncentred boundary conditions (or continualized boundary conditions), according to Eq. (5.4) are: $\kappa_{m/(2n)} = \kappa_{m+m/(2n)} = 0$ and $\alpha_{m/(2n)} = \alpha_{m+m/(2n)} = 0$. We can make use of the result for the centred boundary conditions as $\beta \to \beta$, $\theta_0 \to \theta_{m/(2n)}$, $\kappa_0 \to \kappa_{m/(2n)}$, $\gamma_0 \to \gamma_{m/(2n)}$ and $\alpha_0 \to \alpha_{m/(2n)}$. Then, Eq. (5.5) is numerically iterated backwards to obtain the initial values for the uncentered boundary conditions, θ_0, κ_0, γ_0 and α_0. Figure 10 shows the bifurcation diagram of the second-order gradient elasticity model Eq. (5.2) with uncentred boundary conditions Eq. (5.4) for $n = 4$, and that of the *Hencky* chain of 4 links. Solutions where the relative rotation between neighbouring links of the *Hencky* chain exceeds 2π are not shown. Figure 11 shows the first three paths of the the *Hencky* chain and the first three paths of the second-order gradient elasticity model Eq. (5.2) with uncentred boundary conditions Eq. (5.4) for $n = 4$. These results are calculated using the numerical outcomes for the second-ordered gradient elasticity model with centred boundary conditions. It is worth noting that the second bifurcated branch of the original model with centred boundary conditions (Figure 9) disappears as the uncentred boundary conditions are introduced (Figure 11). This path can be regarded as a parasitic solution that vanishes as the boundary conditions are uncentred. Hence, the third and fourth paths of the previous model become the second and third paths of the current model. Comparing Figures 9 and 11 suggests that the second-order gradient elasticity model with uncentred boundary conditions approximates the *Hencky* chain better than the second-order gradient elasticity model with centred boundary conditions.

A closed-form solution of the buckling load can be also obtained for the second-order gradient *elastica* with centred or uncentred boundary conditions. For centred boundary conditions, the buckling mode can be obtained as:

$$\theta(\xi) = \theta_0 \cos \pi\xi \;\Rightarrow\; \beta = \pi^2\Big(1 - \pi^2 \frac{l_c^2}{L^2}\Big) \quad \text{with} \quad l_c^2 = \frac{a^2}{12}$$

whereas for uncentred boundary conditions, the buckling mode is similar to the one of the discrete problem that has been continualized, and leads to the same buckling load obtained with the centred boundary conditions:

$$\theta(\xi) = \theta_0 \frac{\cos\left[\pi\left(\xi - \frac{a}{2L}\right)\right]}{\cos\frac{\pi a}{2L}} \;\Rightarrow\; \beta = \pi^2\Big(1 - \pi^2 \frac{l_c^2}{L^2}\Big) \quad \text{with} \quad l_c^2 = \frac{a^2}{12}$$

6. Fourth-order gradient elasticity models

The fourth-order gradient elasticity model Eq. (3.2) is governed by the following higher-order differential equation:

$$\frac{d^2\theta}{d\xi^2} + \frac{1}{12n^2}\frac{d^4\theta}{d\xi^4} + \frac{1}{360n^4}\frac{d^6\theta}{d\xi^6} = -\beta \sin\theta \tag{6.1}$$

The centred boundary conditions of this fourth-order gradient elasticity model are:

$$\theta'(0) = \theta'(L) = 0, \quad \theta'''(0) = \theta'''(L) = 0 \quad \text{and} \quad \theta^{(5)}(0) = \theta^{(5)}(L) = 0 \tag{6.2}$$

These conditions may be derived from variational arguments starting from the functional:

$$U = \int_0^L \frac{EI}{2}\left(\theta'^2 - \frac{a^2}{12}\theta''^2 + \frac{a^4}{360}\theta'''^2\right) - P(1-\cos\theta)dx$$

The stationarity of this energy functional $\delta U = 0$ also leads to the same nonlinear differential equations Eq. (3.2) with the following higher-order boundary conditions:

$$\left[\left(EI\frac{a^4}{360}\theta'''\right)\delta\theta''\right]_0^L + \left[\left(-EI\frac{a^2}{12}\theta'' - EI\frac{a^4}{360}\theta^{(4)}\right)\delta\theta'\right]_0^L + \left[EI\left(\theta' + \frac{a^2}{12}\theta''' + \frac{a^4}{360}\theta^{(5)}\right)\delta\theta\right]_0^L = 0 \tag{6.3}$$

Note also that the natural boundary condition in Eq. (6.3) may define the bending moment as:

$$M = EI\left(\theta' + \frac{a^2}{12}\theta''' + \frac{a^4}{360}\theta^{(5)}\right)$$

which is identical to Eq. (1.3). Following the reasoning of the second-order gradient elasticity model, the uncentred boundary conditions of this fourth-order gradient elasticity model are:

$$\theta'\left(\frac{a}{2}\right) = \theta'\left(L+\frac{a}{2}\right) = 0 \quad \text{and} \quad \theta'''\left(\frac{a}{2}\right) = \theta'''\left(L+\frac{a}{2}\right) = 0 \quad \text{and} \quad \theta^{(5)}\left(\frac{a}{2}\right) = \theta^{(5)}\left(L+\frac{a}{2}\right) = 0 \tag{6.4}$$

The differential equation of the fourth-order gradient elasticity model, Eq. (6.1), can be transformed in six first order ordinary differential equations using the *Cauchy* reformulation:

$$\begin{aligned}
\theta' &= \kappa \\
\kappa' &= \gamma \\
\gamma' &= \alpha \\
\alpha' &= \varphi \\
\varphi' &= \omega \\
\omega' &= -360n^4(\gamma + 1/12/n^2\varphi + \beta\sin\theta)
\end{aligned} \tag{6.5}$$

This ODE system, written in the short form $\underline{x}' = \underline{f}(\underline{x})$, where $\underline{x} = [\theta, \kappa, \gamma, \alpha, \varphi, \omega]^T$, can be solved numerically with the simplex algorithm, similarly to the case of the second-order gradient elasticity models.

For centred boundary conditions, according to the close-end centered boundary conditions Eq (6.2), $\kappa_0 = 0$, $\alpha_0 = 0$, and $\omega_0 = 0$. There is one parameter, the load β, and there are three variables, θ_0, γ_0, and φ_0. They span a 4D global representation space. For each point in this space Eq. (6.5) can be solved by the predictor-corrector time-stepping algorithm, where the dimensionless, unit rod length is discretized in m parts. It yields the far-end values of θ, γ, and φ. Owing to the far-end centered

boundary conditions, Eq. (6.2), $\kappa_m = 0$, $\alpha_m = 0$, and $\omega_m = 0$ should fulfill, and these are the error functions of the simplex algorithm. In this case, only the first three post-buckling paths are searched for with the simplex path following algorithm. Figure 12 shows the first three paths of the *Hencky* chain and the first three paths of the fourth-order gradient elasticity model Eq. (6.1) with centred boundary conditions Eq. (6.2) for $n = 4$.

For the continualized uncentred boundary conditions, according to Eq. (6.4), the boundary conditions are: $\kappa_{m/(2n)} = \kappa_{m+m/(2n)} = 0$, $\alpha_{m/(2n)} = \alpha_{m+m/(2n)} = 0$, and $\omega_{m/(2n)} = \omega_{m+m/(2n)} = 0$. The result for the centred boundary conditions can be utilized as $\beta \to \beta$, $\theta_0 \to \theta_{m/(2n)}$, $\kappa_0 \to \kappa_{m/(2n)}$, $\gamma_0 \to \gamma_{m/(2n)}$, $\alpha_0 \to \alpha_{m/(2n)}$, and $\varphi_0 \to \varphi_{m/(2n)}$. Eq. (6.5) is iterated backwards to obtain the initial values for the uncentered boundary conditions, θ_0, κ_0, γ_0, α_0, and φ_0.

In this case also the first three post-buckling paths are detailed. Figure 13 shows the first three paths of the *Hencky* chain and the first three paths of the fourth-order gradient elasticity model Eq. (6.1) with uncentred boundary conditions Eq. (6.4) for $n = 4$.

A closed-form solution of the buckling load can be also obtained for the fourth-order gradient *elastica* with centred or uncentred boundary conditions. For centred boundary conditions, the buckling mode can be obtained as:

$$\theta(\xi) = \theta_0 \cos \pi\xi \;\Rightarrow\; \beta = \pi^2 \Big(1 - \frac{\pi^2}{12n^2} + \frac{\pi^4}{360n^4}\Big)$$

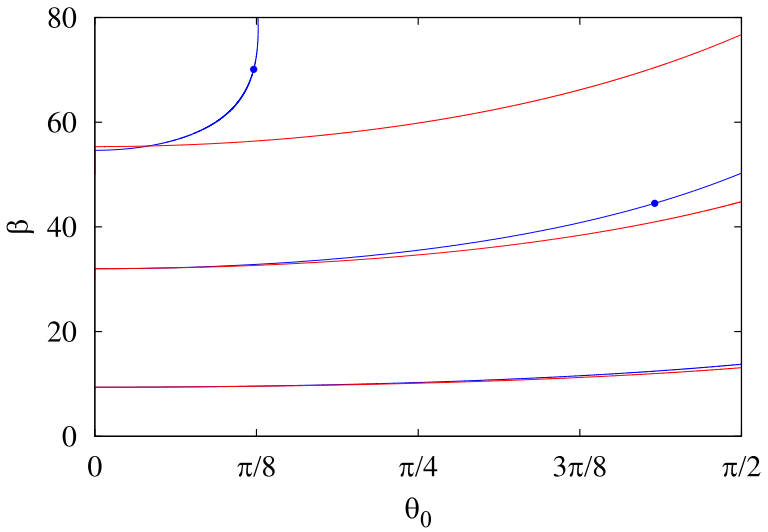

FIGURE 12. The first three paths of the the *Hencky* chain (blue) and the first three paths of the fourth-order gradient elasticity model with centred boundary conditions (red) for $n = 4$. Bifurcation points of the paths are denoted.

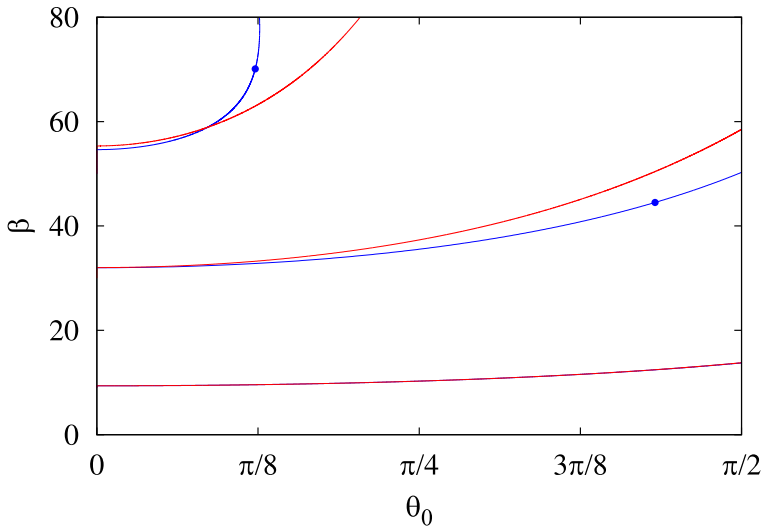

FIGURE 13. The first three paths of the the *Hencky* chain (blue) and the first three paths of the fourth-order gradient elasticity model with uncentred boundary conditions (red) for $n = 4$. Bifurcation points of the paths are denoted.

whereas for uncentred boundary conditions, the buckling mode is similar to the one of the discrete problem that has been continualized, and leads to the same buckling value obtained with the centred boundary conditions:

$$\theta(\xi) = \theta_0 \frac{\cos\left[\pi\left(\xi - \frac{a}{2L}\right)\right]}{cos\frac{\pi a}{2L}} \;\Rightarrow\; \beta = \pi^2\left(1 - \frac{\pi^2}{12n^2} + \frac{\pi^4}{360n^4}\right)$$

Table 1 summarizes the results obtained for the first stable bifurcation branch of the nonlocal *elastica* (Challamel et al. [13]) with local and nonlocal boundary conditions, that of the second-order gradient elasticity model, Eq. (5.2), with centred and uncentred boundary conditions, Eq. (5.3) and Eq. (5.4), and that of the fourth-order gradient elasticity model Eq. (6.1), with centred and uncentred boundary conditions Eq. (6.2) and Eq. (6.4) for $n = 4$.

7. Concluding Remarks

In this paper, higher-order gradient elasticity models have been developed from a geometrically nonlinear lattice system. The discrete *elastica* (Hencky chain) served as a reference model for calibration of the quasi-continuum models. We then tried to capture the main bifurcation branches of the discrete system using an equivalent nonlocal continuum. The quasi-continuum, classified as nonlocal or gradient elasticity continuum, is built from the discrete equations (nonlinear difference equations) by using a continualization method.

It has been shown that neither the nonlocal nor the gradient models are able to capture the overall complex post-buckling nature of the Hencky chain, which is the source of spatially chaotic behavior of the discrete system. However, the first bifurcated branch of the discrete *elastica*, which may be of primary interest for engineering applications, can be efficiently approximated by the nonlocal or the gradient *elastica* even for large rotation values. The higher-order gradient elasticity models are also shown to be efficient for capturing the scale effect of some higher-order post-buckling branches. However, we keep in mind that the prize for the accuracy of the higher-order gradient elasticity models is the additional computational cost due to the higher order of the differential equation that needs to be solved.

Acknowledgment

The work of A. Kocsis was supported by the János Bolyai Research Scholarship of the Hungarian Academy of Sciences.

References

1. I. V. Andrianov, J. Awrejcewicz, O. Ivankov, *On an elastic dissipation model as continuous approximation for discrete media*, Math. Probl. Eng. **2006** (2006), 27373, 1–8.
2. I. V. Andrianov, J. Awrejcewicz, D. Weichert, *Improved continuous models for discrete media*, Math. Probl. Eng. **2010** (2010), 986242, 1–35.
3. S. S. Antman, *Nonlinear problems of elasticity*, Springer, 1995.
4. H. Askes, A. S. J. Suiker, L. J. Sluys, *A classification of higher-order strain-gradient models - linear analysis*, Arch. Appl. Mech. **72** (2002), 171–188.
5. T. M. Atanackovic, *Stability theory of elastic rods*, Ser. Stab. Vib. Control Syst., Ser. A, 1997.
6. T. M. Atanackovic, B. N. Novakovic, Z. Vrcelj, *Application of Pontryagin's principle to bimodal optimization of nanorods*, Int. J. Struct. Stab. Dyn. **12**(3) (2012), 1250012, 1–11.
7. M. Bergou, M. Wardetzky, S. Robinson, B. Audoly, E. Grinspun, *Discrete elastic rods*, ACM Trans. On Graphics **27**(3) (2008), 63:1–63:12.
8. M. Born, *Stabilität der elastischen Linie in Ebene und Raum*, PhD Thesis, Göttingen, Germany, 1906.
9. O. M. Braun, Y. S. Kivshar, *The Frenkel-Kontorova model - Concepts, Methods and Applications*, Springer, 2004.
10. A. M. Bruckstein, R. J. Holt, A. N. Netravali, *Discrete elastica*, Appl. Anal., Int. J. **78**(3–4) (2001), 453–485.
11. N. Challamel, C. M. Wang, I. Elishakoff, *Discrete systems behave as nonlocal structural elements: bending, buckling and vibration analysis*, Eur. J. Mech., A, Solids **44** (2014), 125–135.
12. N. Challamel, V. Picandet, B. Collet, T. Michelitsch, I. Elishakoff, C. M. Wang, *Revisiting finite difference and finite element methods applied to structural mechanics within enriched continua*, Eur. J. Mech. A/Solids, **53** (2015), 107–120.
13. N. Challamel, A. Kocsis, C. M. Wang, *Discrete and nonlocal elastica*, Int. J. Non-linear Mech. **77** (2015), 128–140.
14. G. Domokos, *Qualitative convergence in the discrete approximation of the Euler problem*, Mech. Struct. Mach. **21**(4) (1993), 529–543.
15. G. Domokos, P. Holmes, *Euler's problem, Euler's method, and the standard map; or, the discrete charm of buckling*, J. Nonlinear Sci. **3** (1993), 109–151.
16. G. Domokos, Zs. Gáspár, *A global, direct algorithm for path-following and active static control of elastic bar structures*, Mech. Struct. Mach. **23** (1995), 549–571.
17. M. S. El Naschie, C. W. Wu, A. S. Wifi, *A simple discrete element method for the initial postbuckling of elastic structures*, Int. J. Num. Meth. Eng. **26** (1988), 2049–2060.

18. A. C. Eringen, *On differential equations of nonlocal elasticity and solutions of screw dislocation and surface waves*, J. Appl. Phys. **54** (1983), 4703–4710.
19. L. Euler, *Methodus inveniendi lineas curvas maxima minimive proprietate gaudentes Additamentum I*, De Curvis Elasticis, Lausanne and Geneva, 1744.
20. L. Euler, Sur la force des colonnes, Mem. Acad. Sc. Berlin **13** (1759), 252–282.
21. E. Fermi, J. Pasta, S. Ulam, *Studies of non linear problems, Los Alamos Report LA-1940*, 1955 - Published later in Collected papers of Enrico Fermi, E. Segré (eds.), University of Chicago Press, 1965.
22. R. Frisch-Fay, *Flexible Bars*, Butterworths, London, 1962.
23. Z. Gáspár, G. Domokos, *Global investigation of discrete models of the Euler buckling problem*, Acta Technica Acad. Sci. Hung. **102** (1989), 227–238.
24. Zs. Gáspár, G. Domokos, I. Szeberényi, *A parallel algorithm for the global computation of elastic bar structures*, CAMES **4** (1997), 55–68.
25. S. Goldberg, *Introduction to difference equations with illustrative examples from economics, psychology and sociology*, Dover Publications, New-York, 1958.
26. E. Hairer, S.P. Nørsett, G. Wanner, *Solving Ordinary Differential Equations I: Nonstiff Problems*, 2nd ed., Springer-Verlag, Berlin, 1993.
27. H. Hencky, *Über die angenäherte Lösung von Stabilitätsproblemen im Raummittels der elastischen Gelenkkette*, Der Eisenbau **11** (1920), 437–452. (in German)
28. A. Kocsis, G. Károlyi, *Buckling under nonconservative load: Conservative spatial chaos*, Periodica Polytechnica-Civil Engineering, **49**(2) (2005), 85–98.
29. A. Kocsis, G. Károlyi, *Conservative spatial chaos of buckled elastic linkages*, Chaos **16**(3) (2006), 033111, 1–7.
30. A. Kocsis, *An equilibrium method for the global computation of critical configurations of elastic linkages*, Comput. Struct. **121** (2013), 50–63.
31. A. Kocsis, *Buckling Analysis of the Discrete Planar Cosserat Rod*, Int. J. Struct. Stab. Dyn. **16**(1) (2016), 1450111, 1–29.
32. M. D. Kruskal, N. J. Zabusky, *Stroboscopic perturbation for treating a class of nonlinear wave equations*, J. Math Phys. **5** (1964), 231–244.
33. V. V. Kuznetsov, S. V. Levyakov, *Complete solution of the stability problem for elastic of Euler's column*, Int. J. Non-linear Mech. **37** (2002), 1003–1009.
34. J. L. Lagrange, *Sur la figure des colonnes*, Misc. Taurinensia **5**, 1770–1773 also available in: Oeuvres de Lagrange **2**, Gauthier-Villars, Paris, 1868, pp. 125–170.
35. J. L. Lagrange, *Mécanique Analytique*, Paris, 1788; third ed. In: Mallet-Bachelier, Gendre et successeur de Bachelier, Imprimeur-Libraire du bureau des longitudes, de l'école Polytechnique de l'école centrale des arts et manufactures, Paris, 1853, p. 367.
36. K. A. Lazopoulos, *Post-buckling problems for long elastic beams*, Acta Mech. **164** (2003), 189–198.
37. A. E. H. Love, *A treatise on the mathematical theory of elasticity, 4th Ed.*, Dover Publications, New-York, 1944.
38. G. A. Maugin, *Nonlinear Waves in Elastic Crystals*, Oxford University Press, 1999.
39. W. A. Oldfather, C. A. Ellis, D. M. Brown, *Leonhard Euler's elastic curves*, Isis **20**(1) (1933), 72–160.
40. S. Papargyri-Beskou, K. G. Tsepoura, D. Polyzos, D. E. Beskos, *Bending and stability analysis of gradient elastic beams*, Int. J. Solids Struct. **40** (2003), 385–400.
41. J. Peddieson, G. G. Buchanan, R. P. McNitt, *Application of nonlocal continuum models to nanotechnology*, Int. J. Eng. Sci. **41** (2003), 305–312.
42. P. Rosenau, *Dynamics of nonlinear mass-spring chains near the continuum limit*, Phys. Lett., A **118**(5) (1986), 222–227.
43. P. Rosenau, *Dynamics of dense lattices*, Phys. Rev., B **36** (1987), 5868–5876.
44. H. S. Shen, *Nonlinear analysis of lipid tubules by nonlocal beam model*, J. Theor. Biol. **276** (2011), 50–56.
45. Yu. I. Shokin, *The Method of Differential Approximation*, Springer, 1983.

46. I. K. Silverman, *Discussion on the paper of "Salvadori M. G., Numerical computation of buckling loads by finite differences, Trans. ASCE, 116, 590–636, 1951."*, Trans. ASCE, **116** (1951), 625–626.
47. K. Sogo, *Variational discretization of Euler's elastica problem*, J. Phys. Soc. Japan **75** (2006), 064007.
48. L. J. Sudak, *Column buckling of multiwalled carbon nanotubes using nonlocal continuum mechanics*, J. Appl. Phys. **294** (2003), 7281–7287.
49. N. Triantafyllidis, S. Bardenhagen, *On higher order gradient continuum theories in 1-D nonlinear elasticity. Derivation from and comparison to the corresponding discrete models*, J. Elasticity **33**(3) (1993), 259–293.
50. C. M. Wang, Y. Xiang, S. Kitipornchai, *Postbuckling of nano rods/tubes based on nonlocal beam theory*, Int. J. Appl. Mech. **1**(2) (2009), 259–266.
51. C. M. Wang, Z. Zhang, N. Challamel, W. H. Duan, *Calibration of Eringen's small length scale coefficient for initially stressed vibrating nonlocal Euler beams based on microstructured beam model*, J. Phys. D, Appl. Phys. **46** (2013), 345501.
52. C. T. Wang, *Discussion on the paper of "Salvadori M. G., Numerical computation of buckling loads by finite differences"*, Trans. ASCE **116** (1951), 629–631.
53. C. T. Wang, *Applied Elasticity*, McGraw-Hill, New-York, 1953.
54. C. Y. Wang, *Stability and post buckling of articulated columns*, Acta Mech. **166** (2003), 131–139.
55. J. A. D. Wattis, *Quasi-continuum approximations to lattice equations arising from the discrete non-linear telegraph equation*, J. Phys. A, Math. Gen. **33** (2000), 5925–5944.
56. S. P. Xu, M. R. Xu, C. M. Wang, *Stability analysis of nonlocal elastic columns with initial imperfection*, Math. Probl. Eng. **2013** (2013), 341232, 12p.

ГРАДИЈЕНТНИ ЕЛАСТИЧНИ МОДЕЛИ ВИШЕГ РЕДА ПРИМЕЊЕНИ НА ГЕОМЕТРИЈСКИ НЕЛИНЕАРНИ ДИСКРЕТНИ СИСТЕМ

Резиме. Разматрано је понашање у извијању и после извијања нелинеарног дискретног система на решетки - дискретне еластике. Нелинеарност у суштини долази од геометријског ефекта, док се конститутивни закон сваке компоненте своди на линеарну еластичност. Чланак се првенствено фокусира на релевантност апроксимација вишег реда диференцних једначина континиуумом, тзв. континиуализацији модела решетке. Псеудо-диференцијални оператор једначина решетке се развије у Тејлоров ред, до другог или четвртог реда, што доводи до еквивалентног градијентно еластичног модела другог или четвртог реда. Тачност сваког од ових модела је поређена у односу на почетни модел решетке и у односу на неке друге методе апроксимација засноване на основу рационалног проширења псеудо-диференцијалног оператора. Како се и очекивало, утврђено је да што је изабран виши ниво скраћивања, да је добијена боља тачност у односу на решење базирано на моделу решетке. Овај чланак такође описује кључну улогу коју имају гранични услови, који се такође требају доследно континиуализирати из њихових дискретних израза. Закључено је да модел градијента еластичности вишег реда ефикасно описује ефекте скалирања модела решетке.

Laboratoire d'Ingénierie des MATériaux de Bretagne
Université de Bretagne Sud
Lorient
France
noel.challamel@univ-ubs.fr

Department of Structural Mechanics
Budapest University of Technology and Economics, and
Robert Bosch Kft
Budapest
Hungary
kocsis@ep-mech.me.bme.hu

Engineering Science Programme and Department of Civil and Environmental Engineering
National University of Singapore
Singapore
ceewcm@nus.edu.sg

(Received 13.10.2015)
(Revised 02.11.2015)